Acta Cryst. (1998). D**54**, 347–354

Structure of Azurin I from the Denitrifying Bacterium *Alcaligenes xylosoxidans* NCIMB 11015 at 2.45 Å Resolution

CHUNMIN LI,[a] TSUYOSHI INOUE,[a] MASAHARU GOTOWDA,[a] SHINICHIRO SUZUKI,[b] KAZUYA YAMAGUCHI,[b] KUNISHIGE KAI[b] AND YASUSHI KAI[a]*

[a]*Department of Applied Chemistry, Faculty of Engineering, Osaka University, Suita, Osaka 565, Japan, and* [b]*Department of Chemistry, Faculty of Science, Osaka University, Toyonaka 560, Japan.* *E-mail: kai@chem.eng.osak-u.ac.jp*

(*Received 1 November 1996; accepted 7 August 1997*)

Abstract

Azurin I from *Alcaligenes xylosoxidans* NCIMB 11015 (AzN-I) was crystallized by using PEG 4000 as a precipitant. The crystals belong to the monoclinic crystal system and have a space group $C2$ with the unit-cell parameters of a = 130.67, b = 54.26, c = 74.55 Å, and β = 95.99°. The structure of AzN-I has been solved by the molecular replacement method. Azurin II from the same bacterium (AzN-II) was chosen as the initial structural model. The final crystallographic R value is 17.3% and free R value is 23.6% for 10 958 reflections at a resolution of 2.45 Å. The root-mean-square deviations for main-chain atoms range between 0.19 and 0.26 Å among the four independent molecules in the asymmetric unit. The Cu atom is coordinated to Nδ of His46 and His117 at 2.0 (1) and 1.9 (1) Å, and to Sγ of Cys112 at 2.2 (1) Å, while the carbonyl O atom of Gly45 and Sδ of Met121 coordinate axially to Cu atom at 2.5 (1) and 3.1 (1) Å, respectively. The Cu—N and Cu—S distances of AzN-I are quite similar to those of AzN-II, however, the Cu—O (Gly45) bond length in AzN-I is 0.25 Å shorter than its counterpart in AzN-II. The results have been used to discuss the differences in the spectra of these two proteins.

1. Introduction

Azurins belong to the type I copper protein family (cupredoxins), which are characterized by a very intense absorption band in the visible spectra (λ_{max} = 595–630 nm, $e \simeq 5000\ M^{-1}\,cm^{-1}$), unusually high redox potentials (240–400 mV), and a narrow hyperfine splitting in the electron paramagnetic resonance spectra ($A_{||} \simeq 0.006\ cm^{-1}$) (Gray & Solomon, 1981; Adman, 1991; Sykes, 1991). These monomeric proteins are of molecular mass about 14 kDa and function in electron transfer in photosynthesis and respiratory systems in biological organisms (Ryden, 1984; Adman, 1985). Although it is believed to accept an electron from cytochrome c_{551} and to deliver the electron to nitrite reductase (Antonini *et al.*, 1970; Wilson *et al.*, 1974; Farver *et al.*, 1982; Zumft *et al.*, 1987; Dodd, Hasnain, Abraham *et al.*, 1995), the details of the electron-transfer pathway are still unclear. Crystallographic studies and mutagenesis of azurins have been carried out extensively to investigate the structure of the active site, to explain their unique properties, and to conclude the electron-transfer theory. It is revealed that the azurin molecules consist of a short α-helix and eight β-strands. The Cu atom lies about 7 Å below the surface. It is coordinated by Nδ of His46 and His117, Sγ of Cys112 in a distorted trigonal geometry, while the carbonyl O atom of Gly45 and Sδ of Met121 coordinate axially to it, respectively (Adman & Jensen, 1981; Korszun, 1987; Baker, 1988; Nar *et al.*, 1991*a*; Inoue *et al.*, 1994; Dodd, Hasnain, Abraham *et al.*, 1995). The absolute requirement for a blue site is Cys112 (Mizoguchi *et al.*, 1992). The histidine ligands are also important. Kinetic studies of azurin mutants suggest that the hydrophobic patch on the surface around copper ligand His117 plays a key role in the electron-transfer reaction with cytochrome c_{551} (Van de Kamp, Floris *et al.*, 1990; Van de Kamp, Silestrini *et al.*, 1990). The result was further emphasized by the crystal structure analyses of azurins (Baker, 1988; Nar *et al.*, 1991*a*; Dodd, Hasnain, Abraham *et al.*, 1995). A highly ordered water molecule was revealed to make a hydrogen bond to the Nε of His117 and thus could be part of a short through-bond electron pathway from the copper site to the external surface of the protein. Met121 is not absolutely essential for the blue site, however, it is still important in stabilizing the conformation around the copper and thereby to facilitate the exchange of the electron (Gray & Malmström, 1983; Danielsen *et al.*, 1995). Except the active site, another surface region around His35, the so-called His35 patch was studied extensively. Although it is not in the electron pathway in the azurin cytochrome redox reaction, it exerts nevertheless an influence on the copper site by tuning its

Table 1. *The statistics of data collection*

Resolution	Observed	Theoretical	(%)	R_{merge}	Cumulative values Observed	Theoretical	(%)	R_{merge}
15.00	67	102	65.7	8.0	67	102	65.7	8.0
10.00	199	224	88.8	3.7	266	326	81.6	4.5
7.50	383	415	92.3	4.2	649	741	87.6	4.3
5.00	1577	1671	94.4	5.6	2226	2412	92.3	5.1
3.50	4277	4448	96.2	7.0	6503	6860	94.8	6.3
3.00	3705	3927	94.3	9.6	10208	10787	94.6	6.7
2.75	2918	3135	93.1	11.9	13126	13922	94.3	6.8
2.50	4155	4548	91.4	13.6	17281	18470	93.6	7.0
2.45	904	1087	83.2	13.7	18185	19557	93.0	7.0

redox potential. It was also found that azurin from *P. aeruginosa* displays a pH-dependent conformational change involving the His34 side chain (Nar *et al.*, 1991*b*).

Recently, two azurins were isolated instead of the single previously identified one in both *A. xylosoxidans* NCIMB 11015 and GIFU 1051 (Yamaguchi *et al.*, 1995; Dodd, Hasnain, Abraham *et al.*, 1995). They are named azurin I and azurin II (AzN-I and AzN-II for azurins from *A. xylosoxidans* NCIMB 11015, AzG-I and AzG-II for azurins from *A. xylosoxidans* GIFU 1051). There are some precedents for the synthesis of two azurins in a single bacterial strain. Two distinct azurins were produced in *Methylomonas J.* growing on methylamine (Ambler & Tobari, 1989). Only one of them can accept electrons from the methylamine dehydrogenase. No further studies about the three-dimensional structures and electron-transfer mechanism were reported for these two azurins. AzN-II has an sequence homology of 68.2% to that of AzN-I. Although the absorption spectra of both AzN-I and AzN-II display two peaks at 279 and 620 nm, the molar absorption coefficient (ε_{279} = 10 700 M^{-1} cm^{-1}) of AzN-I at 279 nm is considerably smaller than that (ε_{279} = 14 500 M^{-1} cm^{-1}) of AzN-II. Moreover, the CD spectrum of AzN-I is clearly distinguishable from that of AzN-II. The positive sharp CD band at 291 nm of AzN-I is not observed in AzN-II, and the CD spectrum of AzN-I in the 250–300 nm region is different from that of AzN-II. AzN-I exhibits a stronger band at 610 nm and the 735 nm band shifted to the longer wavelength compared to those of AzN-II. On the other hand, both AzN-I and AzN-II exhibit the same EPR parameters and have almost the same redox potentials. They can donate electrons to purified nitrite reductase under certain experimental conditions. More details of the functions of these two azurins are under investigation. Finding of two azurins from one strain gives a new interest to investigate their structure-function relationship and to explore their electron-transfer mechanism. The crystal structure of AzN-II has been determined at 2.5 Å resolution in 1994 (Inoue *et al.*, 1994) and at 1.9 Å in 1995 (Dodd, Hasnain, Abraham *et al.*, 1995). Here we present our recent work on the crystallization and X-ray structure analysis of AzN-I.

2. Experimental

2.1. *Crystallization, X-ray data collection and processing*

All reagents in the experiment were of chemical grade and used without further purification. The cultivation of *A. xylosoxidans* NCIMB 11015 and purification of AzN-I was carried out by the method previously reported (Yamaguchi *et al.*, 1995). Purified AzN-I was stored at approximately 20 mg ml^{-1} in 0.1 *M* potassium phosphate buffer (pH 6.0) at 277 K. Crystallization was performed using the hanging-drop vapor-diffusion method at 293 K.

Crystals of azurins are usually obtained by the hanging-drop vapor-diffusion method using ammonium sulfate as a precipitant. However, we failed to get the crystals of AzN-I by this method. So other precipitants such as PEG, 2-methyl-2,4-pentanediol (MPD) and the salts of phosphate were screened, and the pH was tested from 4.0 to 9.0. PEG 4000 yielded the most promising crystals over a pH range of 7.5 to 8.5 in Tris–HCl buffer. A 6 µl droplet of 10 mg ml^{-1} AzN-I solution containing 0.1 *M* Tris–HCl buffer (pH 8.0) and 16%(*w*/*v*) PEG was finally set as the hanging drop against 500 µl reservoir solution containing 0.1 *M* Tris–HCl buffer (pH 8.0) and 28%(*w*/*v*) PEG. Needle crystals with maximum dimensions of 0.08 × 0.10 × 2.0 mm appeared in the droplet after 20 d. They are suitable for X-ray crystallographic studies.

The X-ray diffraction data for AzN-I were collected on an R-AXIS IIc image-plate system (Rigaku) using Cu $K\alpha$ radiation (λ = 1.5418 Å) at 293 K, with a crystal-to-detector distance of 130 mm. The crystals did not show any sign of decay during the data collection, so they were stable under the X-ray irradiation. The space group of AzN-I was determined to be monoclinic *C*2 with the unit-cell parameters of a = 130.67, b = 54.26, c = 74.55 Å, and β = 95.99°. Four molecules of AzN-I are

Table 2. *Correlation values for different orientations of the model in the unit cell of AzN-I*

Solution No.	α	β	γ	Correlation coeff.
1	219.0	81.7	167.1	21.9
2	48.8	71.9	161.4	17.0
3	99.4	54.9	175.5	15.1
4	225.9	81.3	22.2	12.4
5	29.7	66.5	166.2	12.2
6	57.3	70.3	8.4	11.8
7	300.8	63.8	−0.8	11.3
8	299.8	44.5	177.8	11.3
9	33.0	72.7	197.3	11.1

included in the asymmetric unit and the volume-to-mass ratio is 2.35 Å^3 Da^{-1}, which is close to the average for the protein crystals reported (Matthews, 1968). The solvent content was calculated to be 47.7% by the use of Matthews' formula. A total of 19 618 reflections were collected (25 frames, 4.5° oscillation, 1 h exposure time for each frame), and these reduced to 11 462 independent reflections with an $R_{\rm merge}$ of 6.9% ($R_{\rm merge} = \sum_h \sum_i |I_{ih} - \langle I_h \rangle| / \sum_h \sum_i \langle I_h \rangle$ where $\langle I_h \rangle$ is the mean intensity of the i observations of reflection h). Image-plate data were processed using the R-AXIS software. Table 1 shows the statistics of data collecton.

2.2. *Structure solution and refinement*

The structure of AzN-I was solved by the molecular-replacement method using *AMoRe* in the *CCP*4 program suite (Collaborative Computational Project, Number 4, 1994). Reflections with $F_o > 1\sigma_F$ were used throughout the molecular replacement and subsequent refinement calculations. The crystal structure of AzN-II refined to an R value of 20.5% at 2.5 Å (Inoue *et al.*, 1994) was chosen as a starting model. The rotation search was carried out from 15 to 3.0 Å resolution. Table 2 shows the correlation values for different orientations of the model in the unit cell of AzN-I. Only the first nine solutions were listed. It implies an unambiguous conclusion that only three molecules are in the asymmetric unit: the first three rotation solutions seem to be the correct ones, the correlation values were 21.9, 17.0 and 15.1, as compared with around 12.0 for all the six remaining solutions. Translation-function searches were then carried out in the same resolution range for the first three rotation solutions. The model of three molecules gives an R factor of 38.7%. However, subsequent refinement of the model by alternating cycles of *X-PLOR* (Brünger, 1992*a*) refinement and manual rebuilding failed. The model was obviously distorted in spite of the decrease in R factor to 21.5%. Furthermore, free R values randomly omitting 10% of the reflections (Brünger, 1992*b*) calculated at every stage of refinement are difficult to improve. They remained at 30.0% although more than 200 water molecules were added.

Table 3. *Final solutions for the four independent molecules in the asymmetric unit*

α	β	γ	Tx	Ty	Tz
217.4	80.6	167.4	0.0907	0.0001	0.1532
47.5	72.4	162.2	0.4234	0.0515	0.6582
301.2	45.5	177.0	0.3245	0.5244	0.3206
99.9	53.5	175.5	0.1679	0.4889	0.8341

Thus, we searched for a fourth molecule from the beginning. Solution 8 in Table 2 was found to be the correct answer although the correlation value was 11.3. The molecular-replacement model of four molecules gave a correlation value of 68.9 and an initial R factor of 34.4%. Table 3 shows the final results.

The molecular-replacement model was subsequently refined using the *X-PLOR* software package (Brünger, 1992*a*) and the model was rebuilt with the *TURBO-FRODO* computer graphics software (Cambillau, 1992). Two different refinement protocols were tested in the initial stage of the refinement. In one of the protocols, four molecules in the asymmetric unit were subjected to the non-crystallographic symmetry (NCS) with effective force constants of 1255 kJ mol^{-1} Å^{-1} (300 kcal mol^{-1} Å^{-2}) for the main-chain atoms and 627.6 kJ mol^{-1} Å^{-1} (150 kcal mol^{-1} Å^{-2}) for the side-chain atoms. In another one, this restraint was not used. Comparison of the models obtained shows the former one is effective to improve the electron-density map and the stereochemical properties of the main chain and the side chains. The starting geometry for the copper site was the average of azurin models reported at high resolution (Baker, 1988; Nar *et al.*, 1991*a*; Dodd, Hasnain, Abraham *et al.*, 1995).

The rigid-body refinement was carried out initially to improve the positional and orientational parameters of the model obtained by molecular-replacement method. At that point, the resolution was gradually increased to 2.45 Å resolution and the R factor was 30.1%. To minimize model bias, the model was subjected to simulated annealing by first heating the system to 4000 K and slowly cooling it to 300 K in a time step of 0.00025 ps. This dropped the R value to 24.3%. Positional parameters and temperature factors were then refined alternatively. A $2F_o - F_c$ Fourier electron-density map was computed at every stage of refinement and the model was adjusted carefully to fit the density map. The R factor was decreased to 19.7% for all data between 8 and 2.45 Å after several rounds of refinement. At that stage, water molecules were added in the places with high $2F_o - F_c$ electron density and reasonable hydrogen-bond contacts using the programs *PEAK* and *WATER* (Okamoto & Hirotsu, unpublished work). They are included in the subsequent refinement.

Table 4. *Statistics of the final model as refined by X-PLOR*

Resolution range (Å)	8–2.45
Final *R* factor	17.3
Free *R* factor	23.6
No. of reflections ($I > I\sigma$)	10958
No. of non-H atoms for refinement	
Protein atoms	4 × 972
Ions	4 × 1
Solvent molecules	81
Average *B* factor (Å^2)	
Main chain	27.2
Side chain	30.9
Solvent	38.2
Gly45	10.5
His46	8.2
Cys112	14.0
His117	14.1
Cu^{II}	17.0
R.m.s.d	
Bond lengths (Å)	0.024
Angle distances (Å)	5.49

When the *B* factor of a solvent molecule exceeded 60 Å^2 or a solvent molecule moved out of density, it was deleted from the model. During this process, all the restraints (restraints of NCS and copper geometry) were removed gradually. As a result, 81 water molecules were added to the atomic coordinates list.

3. Results and discussion

The statistics of the final model is listed in Table 4. The expected atomic coordinate error is estimated to be about 0.25 Å from a Luzzati plot (Fig. 1; Luzzati, 1952). The model stereochemistry was analyzed using the *PROCHECK* suite (Laskowski *et al.*, 1993). A Ramachandran plot (Ramachandran & Sasisekharan, 1968) of the conformational angles of φ/ψ for the four independent molecules is given in Fig. 2. 91.7% of the non-glycine and non-proline residues have conformational angles in the most favored regions and the other 8.3% in additional allowed regions. The main-chain and side-chain properties of the structure, which were described by Laskowski *et al.* (Laskowski *et al.*, 1993), fall either in the 'inside' or BETTER categories indicating that they are in good agreement with other well refined structures. The average *B* factors for main-chain atoms, side-chain atoms, and the solvent molecules are listed in Table 4. Some residues near the C and N terminals (Ala1 and Asp129 of molecule *B*; Ala1, Glu2, Cys3, Leu127, Val128 and Asp129 of molecule *C*; Ala1, Glu2, Cys3, Lys126, Leu127, Val128, Asp129 of molecule *D*), show average *B* factors over 50 Å^2. In addition, the loop residues 22–27 and residues 103–107 of all molecules show relatively large *B* values (49.7–63.7 Å^2) as expected. The electron density was continuous for most part of the polypeptide backbone.

No simple local symmetry relationship for the four independent molecules in the asymmetric unit was found. Superpositions of the main-chain atoms (N, Cα, C, O) of these four molecules by *X-PLOR* (Brünger, 1992*a*) gave the average r.m.s. differences ranging from 0.25 to 0.28 Å, which is near the expected atomic coordinate error value of 0.25 Å estimated from a Luzzati plot. Therefore, the differences among the four molecules are small in general. For the atoms of the β-strands, and the loop around the copper site, the r.m.s. differences are about 0.25 Å and their *B* factors are less than 20 Å^2, indicating the main body of the molecule and the area around the active site are highly conserved.

The final model of AzN-I includes 4 × 129 residues. The fold of the polypeptide chain is similar to that

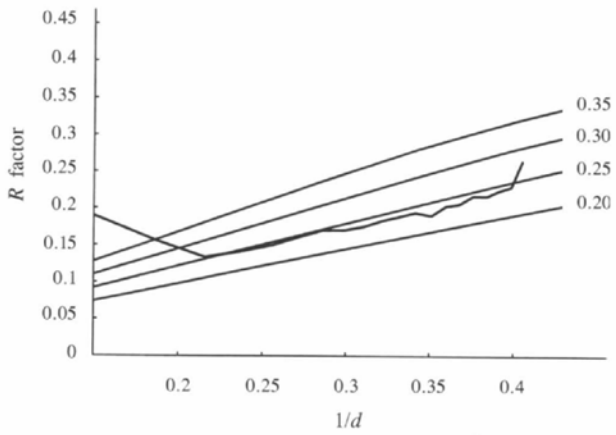

Fig. 1. Luzzati plot of *R versus* resolution for the 2.45 Å refined model of AzN-I.

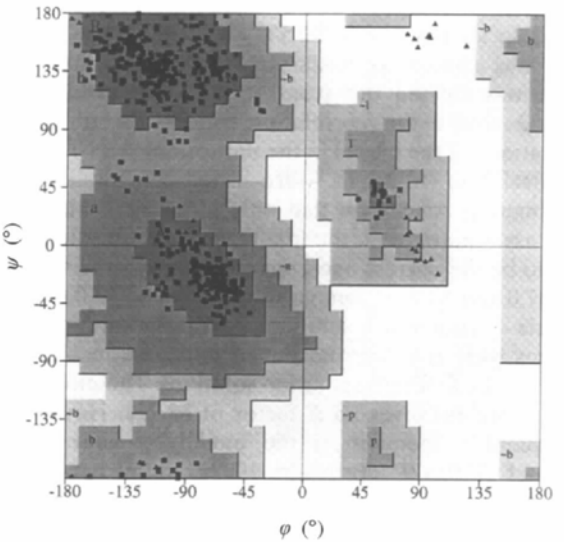

Fig. 2. Ramachandran plot for the refined AzN-I. Energetically favorable regions for the values of φ and ψ are indicated. Glycine residues are indicated by triangles and non-glycine residues by squares.

found in other azurins. It consists of one α-helix and eight β-strands. The sequence homology of AzN-I and AzN-II is 68.2%. So they are expected to have similar three-dimensional structures. The structure of AzN-I was compared with that of AzN-II (Dodd, Hasnain, Abraham *et al.*, 1995) using main-chain atoms (N, Cα, C, O) by *MIDAS* (Ferrin *et al.*, 1988) (Fig. 3. shows the superpositions of AzN-I and AzN-II). There are average displacements of 0.74, 0.75, 0.75 and 0.75 Å between four independent AzN-I molecules and AzN-

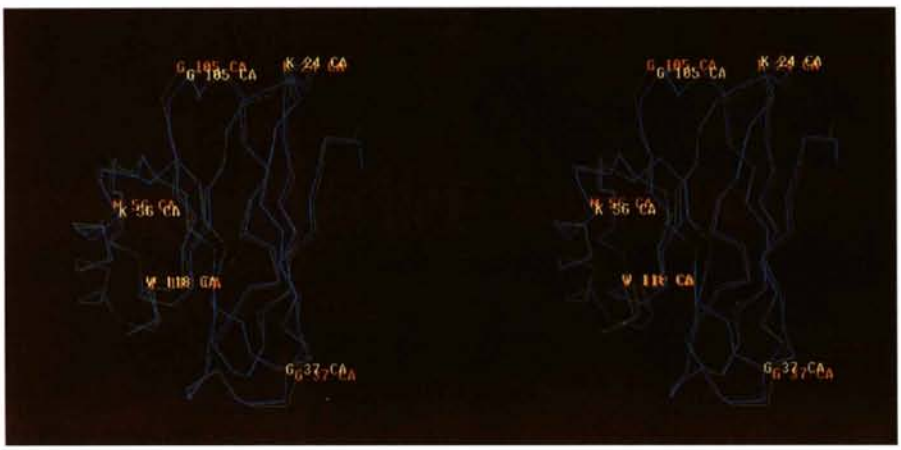

Fig. 3. The superpositions of AzN-I (green colour) and AzN-II (blue colour) using main-chain atoms (N, Cα, C, O) by *MIDAS*.

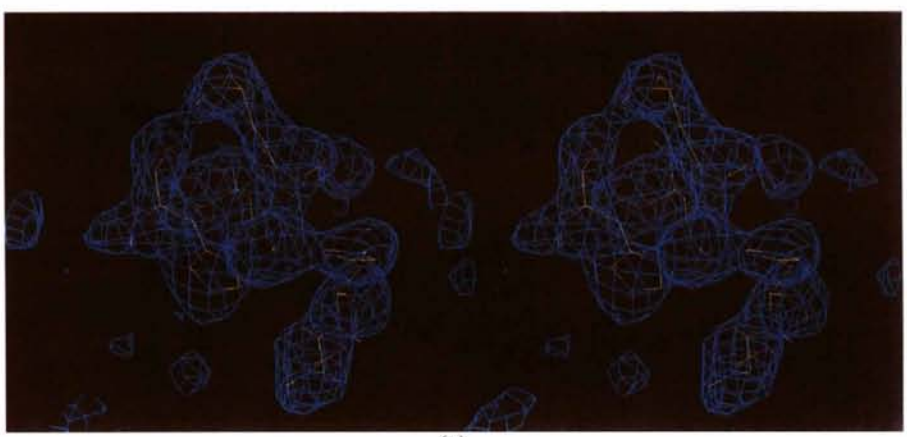

(*a*)

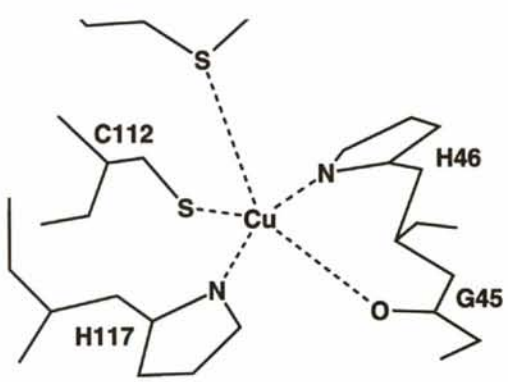

(*b*)

Fig. 4. Copper active site in the refined AzN-I model. (*a*) The stereo $F_o - F_c$ electron-density Fourier map of Cu active site in AzN-I contoured at 1.5σ level with the contribution of Cu and the ligands being omitted. (*b*) Coordination geometry.

II molecules, respectively. The largest differences are near the C and N terminals as expected. The other main differences are in the regions around residues 24, 37, 104 and 118.

Fig. 4(*a*) shows the stereo $F_o - F_c$ electron-density Fourier map of Cu active site in AzN-I contoured at 1.5σ level with the contribution of Cu and the ligands being omitted. Like the case of AzN-II, Nδ of His46 and His117, Sγ of Cys112 of AzN-I coordinate to the Cu atom in a distorted trigonal plane while the carbonyl O atom of Gly45 and Sδ atom of Met121 interact with it axially (Fig. 4*b*). Details of copper geometry are given in Table 5 together with those of AzN-II. While the Cu—N distances of AzN-I are quite similar to those of AzN-II, the Cu—O (Gly45) bond length is 0.25 Å shorter and the Cu—Sδ (Met121) bond length is a little shorter than their counterparts in AzN-II. Even though there may be some errors for the parameters resulted from the low-resolution data, these differences are significant. It has been reported that the length of the Cu—S_{Met} bond in blue copper proteins from diverse sources varies very widely, ranging from 2.62 Å in cucumber basic protein to 3.26 Å in bacterium azurin (Adman, 1991; Sykes, 1991; Dodd, Hasnain, Abraham *et al.*, 1995). The result of a recent quantum chemical calculation shows that the Cu—S_{Met} bond length may change by 0.5 Å around 2.62 Å at a cost of less than 21 kJ mol^{-1} (5 kcal mol^{-1}), which can easily be obtained by hydrogen bonds in the protein (Ryde *et*

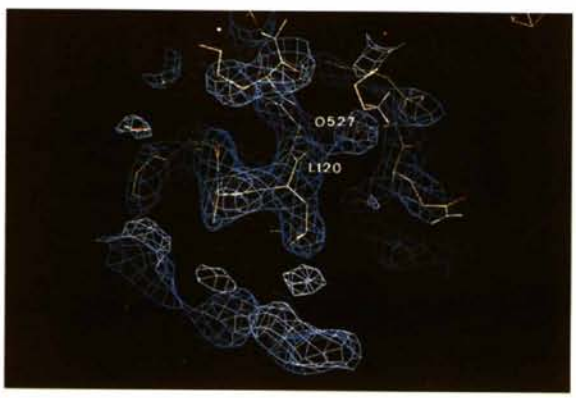

Fig. 5. A water molecule was found to form a hydrogen bond with the O atom of residue 120.

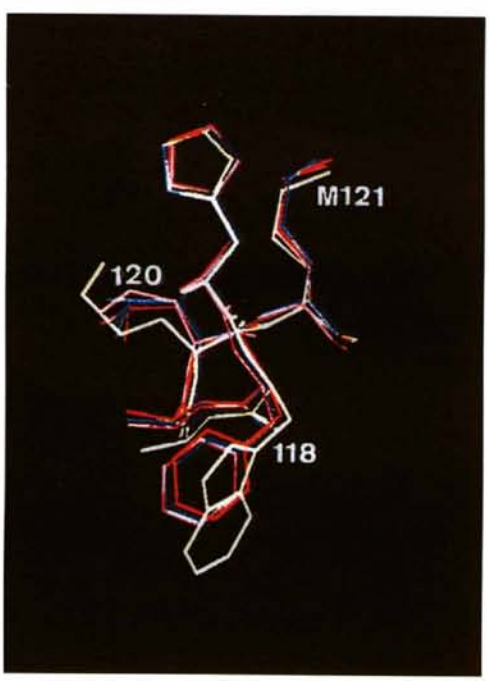

Fig. 6. Region of residues from 117 to 121 after the superposition of the main chain atoms of AzN-I (red, pink, blue and green represent the four independent molecules in the a.u., respectively) and those of AzN-II (white).

Table 5. *The copper site geometry*

Numbers in parentheses give the maximum deviations from average distances and angles, when the average is taken over the four molecules in the asymmetric unit.

	AzN-I	AzN-II†
(*a*) Cu—ligand bond length (Å)		
Cu—Nδ(46)	2.0 (1)	2.02
Cu—Nδ(117)	1.9 (1)	2.02
Cu—Sγ(112)	2.2 (1)	2.12
Cu—O(45)	2.5 (1)	2.75
Cu—Sδ(121)	3.1 (1)	3.26
(*b*) Bond angles around copper (°)		
O(45)—Cu—Sδ(121)	145 (5)	147.41
Nδ(46)—Cu—Sγ(112)	127 (4)	134.03
Nδ(46)—Cu—Nδ(117)	113 (3)	106.36
Sγ(112)—Cu—Nδ(117)	120 (5)	119.59

† Dodd, Hasnain, Abraham *et al.* (1995).

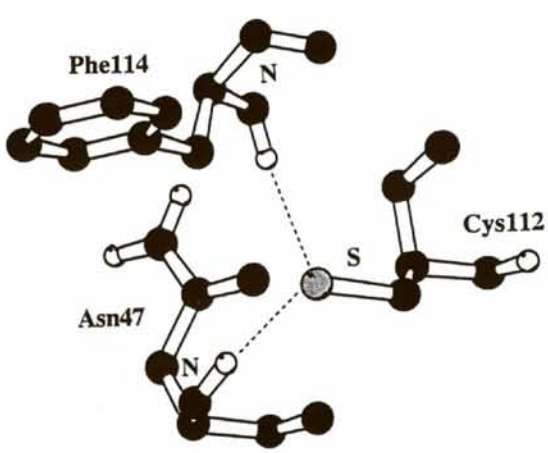

Fig. 7. Interaction between the S atom of Cys112 and the NH groups of residue 114 and residue 47.

al., 1996). So Cu—S_{Met} or Cu—O_{Gly} is usually considered to be extremely sensitive to the charge on the copper ion and the electrostatic properties of the surrounding residues. A water molecule was found to form a hydrogen bond with the O atom of residue 120, which is the neighbor of Met121, for the four monomers, respectively (Fig. 5). The formation of this hydrogen bond may offer energy for a slightly stronger combination of Cu—Sδ (Met121). As mentioned above, the region around residue 118 is significantly different for both proteins. Fig. 6 shows the region from residues 117 to 121 after the superposition of the main-chain atoms of AzN-I and those of AzN-II. From the figure we can see that they are Phe118 and Leu120 in AzN-I instead of Trp118 and Met120 in AzN-II. Apparently they have influenced the copper geometry in both proteins, respectively, and thus made their Cu—O (Gly45) bond lengths different. The stronger Cu—O (Gly45) bond may lower the charge on the copper ion and, therefore, change the coordinations of other ligands, in which Cys112 might be the most sensitive (S has more electrons than N and O). Two N—H···S hydrogen bonds to the S atom of Cys112 involving the NH group of residue 114 and residue 47 were found in AzN-II (Fig. 7). S···H—N (Asn47) is 3.49 Å and S···H—N (Phe114) is 3.57 Å. They may stabilize a more negative S and a stronger Cu—Sγ (Cys112) bond. However, the bond lengths are 3.5 and 3.8 Å in AzN-I, respectively. So the cysteine S in AzN-I can be considered the weak recipient of only one S···H—N bond. For the above reasons, we could then explain why the Cu—O (Gly45) bond length in AzN-I is 0.25 Å shorter than that of AzN-II. It is generally accepted that the bands at 610 and 735 nm are associated with S(Cys)—Cu charge-transfer interaction (Solomon *et al.*, 1980). As we mentioned before, AzN-I exhibits a stronger band at 610 nm and the 735 nm band shifted to the longer wavelength compared to those of AzN-II. We think the shorter Cu—O (Gly45) bond length in AzN-I may be the main reason for the 735 nm band shifting to the longer wavelength and a stronger band at 610 nm of AzN-I compared with that of AzN-II may be the result of the relatively more positivly charged Cu atom because of the total effect of the shorter Cu—O (Gly45) bond length.

4. Concluding remarks

It is very interesting that the organism produces two electron-donor proteins with quite similar properties instead of one. From an evolutionary viewpoint, we believe the organism has its own reasons and there might be some fundamental functional difference between the two proteins which we have not found yet. It is a pity that we cannot refine the structure of AzN-I at high resolution at the moment, so we could not obtain a clear map of the water molecules around the His117 hydrophobic patch to discuss the possible pathway for the electron-transfer and the possible different electron-transfer mechanism for AzN-I and AzN-II. However, the structure determination of AzN-I at 2.45 Å provides the information that the copper geometry of the copper sites of AzN-I and AzN-II are different. It also revealed that the copper site can be affected by the surrounding residues of the protein and further emphasized the fact that Cu—O is sensitive to the electrostatic properties of the surrounding residues. We hope our results can be of help for biochemists to pay more attention to the differences of the two proteins and finally conclude the electron-transfer theory for them.

CL thanks the Yoneyama Rotary Scholarship Foundation in Japan for offering her a studentship.†

References

Adman, E. T. (1985). *Structure and function of small blue copper proteins.* In *Topics in Molecular and Structural Biology: Metalloproteins*, edited by P. M. Harrison, Vol. 6, Part 1, pp. 1–42. Weinheim: Chemie Verlag.

Adman, E. T. (1991). *Adv. Protein Chem.* **43**, 145–197.

Adman, E. T. & Jensen, L. H. (1981). *Isr. J. Chem.* **21**, 8–12.

Ambler, R. P. & Tobari, J. (1989). *Biochem. J.* **261**, 495–499.

Antonini, E., Finazzi-Agro, A., Avigliano, L., Guerrieri, P., Rotilio, G. & Mondovi, B. (1970). *J. Biol. Chem.* **245**, 4847–4856.

Baker, E. N. (1988). *J. Mol. Biol.* **203**, 1071–1095.

Brünger, A. T. (1992*a*). *X-PLOR Manual, Version* 2.1, Yale University, New Haven, CT, USA.

Brünger, A. T. (1992*b*). *Nature (London)*, **355**, 472–475.

Cambillau, C. (1992). *TURBO-FRODO, Molecular Graphics Program for Silicon Graphics IRIS 4D Series, Version* 3.0. Bio-Graphics, Marseille, France.

Collaborative Computational Project, Number 4 (1994). *Acta Cryst.* **D50**, 760–763

Danielsen, E; Bauer, Hemmingsen, L., Andersen, M., Bjerrum, M. J., Butz, T., Tröger, W., Canters, G. W., Hoitink, C. W. G., Karlsson, G., Hansson, Ö. & Messerschmidt, A. (1995). *J. Biol. Chem.* **270**, 573–580.

Dodd, F. E., Hasnain, S. S., Abraham, Z. H. L., Eady, R. R. & Smith, B. E. (1995). *Acta Cryst.* **D51**, 1052–1064

Dodd, F. E., Hasnain, S. S., Hunter, N. N., Abraham, W. N., Debenham, M., Kanzler, H., Eldridge, M., Eady, R. R., Ambler, R. P. & Smith, B. E. (1995). *Biochemistry*, **34**, 10180–10186.

Farver, O., Blatt, Y. & Pecht, I. (1982). *Biochemistry*, **21**, 3556–3561.

† Atomic coordinates and structure factors have been deposited with the Protein Data Bank, Brookhaven National Laboratory (Reference: 1RKR, R1RKRSF). Free copies may be obtained through The Managing Editor, International Union of Crystallography, 5 Abbey Square, Chester CH1 2HU, England (Reference: TS0005).

Ferrin, T. E., Huang, C. C. Jarvis, L. E. & Langridge, R. (1988). *J. Mol. Graphics*, **6**, 13–27.

Gray, H. B. & Malmström, B. G. (1983). *Comments Inorg. Chem.* **2**, 203–209.

Gray, H. B. & Solomon, E. I. (1981). *Electronic Structures of Blue Copper Centers in Proteins*. In *Copper Proteins*, edited by T. Spiro, pp. 1–39. New York: John Wiley & Sons.

Inoue, T., Shibata, N., Nakanishi, H., Koyama, S., Ishii, H., Kai, Y., Harada, S., Kasai, N., Ohshiro, Y., Suzuki, S., Kohzuma, T., Yamaguchi, K., Shidara, S. & Iwasaki, H. (1994). *J. Biochem.* **116**, 1193–1197.

Konnert, J. H. & Hendrickson, W. A. (1980). *Acta Cryst.* A**36**, 344–349.

Korszun, Z. R. (1987). *J. Mol. Biol.* **196**, 413–419.

Laskowski, R. A., MacArthur, M. W., Moss, D. S. & Thornton, J. M. (1993). *J. Appl. Cryst.* **26**, 283–291.

Luzzati, V. (1952). *Acta Cryst.* **5**, 802–810.

Matthews, B. W. (1968). *J. Mol. Biol.* **33**, 491–497.

Mizoguchi, T. J., Di Bilio, A. J., Gray, H. B. & Richards, J. H. (1992). *J. Am. Chem. Soc.* **114**, 10076–10078.

Nar, H., Messerschmidt, A. & Huber, R. (1991). *J. Mol. Biol.* **218**, 427–447.

Nar, H., Messerschmidt, A., Huber, R., Van de Kamp, M. & Canters, G. W. (1991*a*). *J. Mol. Biol.* **221**, 765–772.

Nar, H., Messerschmidt, A., Huber, R., Van de Kamp, M. & Canters, G. W. (1991*b*). *J. Mol. Biol.* **218**, 427–447.

Ramachandran, G. N. & Sasisekharan, V. (1968). *Adv. Protein Chem.* **23**, 238.

Ryde, U., Olsson, M. H. M., Pierloot, K. & Roos, B. O. (1996). *J. Mol. Biol.* **261**, 586–596.

Ryden, L. (1984). *Structure and Evolution of the Small Blue Proteins*. In *Copper Proteins and Copper Enzymes*, edited by R. Lontie, Vol. 1, pp. 157–181. Boca Raton: CRC Press.

Solomon, E. I., Hare, J. W., Dooley, D. M., Dawson, J. H., Stephens, P. J. & Gray, H. B. (1980). *J. Am. Chem. Soc.* **102**, 168–178.

Sykes, A. G. (1991). *Adv. Inorg. Chem.* **36**, 377–408.

Van de Kamp, M., Floris, R., Hali, F. C. & Canters, G. W. (1990). *J. Am. Chem. Soc.* **112**, 907–908.

Van de Kamp, M., Silvestrini, M. C., Brunori, M., Van Beeumen, J., Hali, F. C. & Canters, G. W. (1990). *Eur. J. Biochem.* **194**, 109–118.

Wilson, M., Greenwood, C., Brunori, M. & Antonini, E. (1974). *Biochem. J.* **145**, 449–457.

Yamaguchi, K., Nakamura, D. N., Shidara, S., Iwasaki, H. & Suzuki, S. (1995). *Chem. Lett.* **5**, 353–354.

Zumft, W. G., Gotzmann, D. J. & Kroneck, D. M. H. (1987). *Eur. J. Biochem.* **168**, 301–307.